

Co, Zn and Ag-MOFs evaluation as biocidal materials towards photosynthetic organisms

This version is made available in accordance with publisher policies.

Please, cite as follows:

Keila Martín-Betancor, Sonia Aguado, Ismael Rodea-Palomares, Miguel Tamayo-Belda, Francisco Leganés, Roberto Rosal, Francisca Fernández-Piñas, Co, Zn and Ag-MOFs evaluation as biocidal materials towards photosynthetic organisms, *Science of The Total Environment*, Volume 595, 1 October 2017, Pages 547-555

<https://doi.org/10.1016/j.scitotenv.2017.03.250>

<http://www.sciencedirect.com/science/article/pii/S0048969717307817>

Co, Zn and Ag-MOFs evaluation as biocidal materials towards photosynthetic organisms

Georgiana Amariei¹, Karina Boltes^{1,2,*}, Roberto Rosal^{1,2}, Pedro Letón^{1,2}, Keila Martín-Betancor¹, Sonia Aguado², Ismael Rodea-Palomares¹, Miguel Tamayo-Belda¹, Francisco Leganés¹, Roberto Rosal², Francisca Fernández-Piñas^{1,*}

¹ Department of Biology, Facultad de Ciencias, Universidad Autónoma de Madrid, 28049 Madrid, Spain

² Department of Chemical Engineering, Universidad de Alcalá, Alcalá de Henares, 28871 Madrid, Spain

* Corresponding author: francisca.pina@uam.es

Abstract

In the present study, the biocidal activity of three different metal organic frameworks (MOFs) based on Co (Co-SIM1), Zn (Zn-SIM1) and Ag (Ag-TAZ) has been evaluated towards one green alga and two cyanobacteria. These organisms are present in fresh- and seawater and take part in the early stages of the biofouling process. The biocidal activity of these materials was evaluated by measuring chlorophyll a concentration and by inhibition zone testing. After 24 h of exposure the three different MOFs caused > 50% of chlorophyll a concentration inhibition towards both cyanobacteria, however, although the green alga presented a great sensitivity for Ag-TAZ (reaching 90% of chlorophyll a concentration inhibition), it was much more resistant to the rest of MOFs. Bioavailability of these metals was studied using ICP-MS, the chemical speciation program Visual MINTEQ, and a heavy metal bioreporter bioanalytical tool. We have elucidated that the biocidal activity presented by these MOFs was due to the dissolved metals released from them and more exactly, it depended on the bioavailability presented by these metal ions, which was closely related with the free ion concentration. This article highlights the potential use of different MOFs as biocidal material towards photosynthetic organisms and reveals important differences in the sensitivity between these organisms that should be taken into account in order to increase the biocidal spectrum of these materials.

Keywords: Biocidal material; Heavy metal bioreporter; Metal bioavailability; MOFs; Photosynthetic organisms.

1. Introduction

Metal-organic frameworks (MOFs) are one of the latest developments in nanotechnology (Ferey, 2008; McKinlay *et al.*, 2010; Spokoyny *et al.*, 2009). These new porous inorganic-organic hybrid materials are constructed by controlled crystallization, joining metal-containing units with multifunctional organic ligands. Due to the inherent porous structure of MOFs, changeable surface functional groups and different choice of metal and ligands, different types of MOFs can be developed. Their structure give them great potential for a wide range of applications, such as gas storage, catalysis, chemical sensing, drug delivery (Beg *et al.*, 2016; Furukawa *et al.*, 2013; Getman *et al.*, 2012; Horcajada *et al.*, 2010; Kreno *et al.*, 2012; Kuppler *et al.*, 2009; Yaghi *et al.*, 2003) and the most recent application as biocidal materials (Wyszogrodzka *et al.*, 2016). The use of some MOFs as biocide material in water treatment and biomedical applications has been evaluated (Prince *et al.*, 2014; Quirós *et al.*, 2015). Some advantages of using MOFs based materials instead of traditional chemical disinfectants are their high durability, wide antimicrobial spectrum, high effectiveness and thermal-optical stabilities.

Other porous structures used as biocide material are zeolites or silica based materials. Zeolites are porous crystalline alumina silicate minerals with uniform

molecular-sized pores. They contain metal ions, which can readily be exchanged by other metals such as silver, copper, and zinc ions *via* ion-exchange post-synthesis treatment for their use as antimicrobial agents due to the easily metal ion extraction from the zeolites (Dong *et al.*, 2014; Sánchez *et al.*, 2017; Zhou *et al.*, 2014). Many different kinds of silica-supported materials have been proposed for antimicrobial applications. Basic copper chloride structures supported on silica nanoparticles showed similar antibacterial activity against *Escherichia coli* and *Staphylococcus aureus* than copper-exchanged mordenite zeolite microparticles (Palza *et al.*, 2015). Reduced copper on the surface of spherical silica nanoparticles displayed significant antibacterial ability (Kim *et al.*, 2006). Mesoporous silica has also been used as support for metals because thanks to its high surface area and uniform pore distribution offers the possibility of dispersing metal nanoparticles inside a non-nano support. Copper oxide and reduced silver have been dispersed in the form of nanoparticles inside a highly ordered mesoporous SBA with antifungal and antibacterial activities (Díez *et al.*, 2017; Quirós *et al.*, 2016). The mechanism of zeolite and silica-supported metals is different from that of MOF-based antimicrobials. Whereas zeolites are cation-exchangers and supported metals or oxides must change its oxidation state or dissolve before becoming

bioavailable, MOFs are constructed directly with the desired metal linked by covalent bonds. The structures of MOFs can be designed at the atomic scale by an appropriate choice of metal and organic ligand, which define their antimicrobial activity and allowing a more controlled release of the metal ions. Furthermore, these metals coordination polymers could provide some advantages over the use of nanoparticles (NPs) as biocidal material (Lu *et al.*, 2014).

In the last years, several MOFs have been successfully tested as biocides materials, especially those based on silver (Berchel *et al.*, 2011; Liu *et al.*, 2010; Lu *et al.*, 2014; Rueff *et al.*, 2015). Silver-based biocidal materials are well known for their antimicrobial properties (Egger *et al.*, 2009; Lalueza *et al.*, 2011; Lemire *et al.*, 2013; Matsumura *et al.*, 2003; Rai *et al.*, 2009; Sondi and Salopek-Sondi, 2004). However, silver is an expensive metal and the indiscriminate use of it in many antimicrobial materials is suspected to promote not only a general toxic risk but also bacterial resistance (Blaser *et al.*, 2008; Merlino and Kennedy, 2010).

New MOFs based on different metals such as Co, Zn or Cu have also emerged. In most cases, these MOFs have been successfully tested towards heterotrophic organisms like *Pseudomonas putida*, *E. coli*, *Saccharomyces cerevisiae* or *S. aureus* (Aguado *et al.*, 2014; Wang *et al.*, 2015; Wojciechowska *et al.*, 2012; Zhuang *et al.*, 2012) and to marine bacteria as *Cobetia marina* (Sancet *et al.*, 2013). However, studies to examine the biocidal effect of MOFs to photosynthetic organisms as cyanobacteria or algae are lacking (Wyszogrodzka *et al.*, 2016).

Cyanobacteria and algae are photosynthetic, aquatic organisms present in both freshwater and seawater. As primary producers, they are relevant organisms in these environments; however, along with bacteria, they have other implications also as organisms that take part in the early stages of the biofouling process (Briand, 2009; Mieszkina *et al.*, 2013; Rosenhahn *et al.*, 2010; Salta *et al.*, 2013). Biofouling is the accumulation of microorganisms, algae, plants or/and animals on surfaces, mainly in the aquatic environments with a great economic impact on shipping or water filtration (Nguyen *et al.*, 2012; Schultz *et al.*, 2011). The colonization of these structures by unicellular microorganisms such as bacteria, cyanobacteria, unicellular algae and protozoa is denominated "microfouling" or "slime" and normally constitute the early stage of biofilm formation. For a deeper understanding of the colonization process, see the review by Dang and Lovell (2016) and Rosenhahn *et al.* (2010).

In the present article, we have evaluated the biocidal activity of two zeolite imidazolate frameworks (ZIF), a sub-family of MOFs, consisting of transition metal ions, Co^{2+} and Zn^{2+} , and imidazolate ligands, denominated Co-SIM1 and Zn-SIM1, respectively (Aguado *et al.*, 2010; Aguado *et al.*, 2011;

Farrusseng *et al.*, 2009). Different to their MOF analogues with carboxylates ligands, a number of ZIF exhibit exceptional thermal, hydrothermal and chemical stability (Banerjee *et al.*, 2009; Phan *et al.*, 2010). Furthermore, we analysed one silver-triazole coordination polymer (Ag-TAZ) prepared with a polyazaheteroaromatic compound, 1,2,4-triazole, a well-known intermediate compound of industrial relevance (Haasnoot, 2000), which is also widely used as ligand (Zhang *et al.*, 2005).

The biocidal activity of these three different MOFs towards potential biofouling photosynthetic organisms: one filamentous (*Anabaena* sp. PCC 7120, hereinafter *Anabaena*), and one unicellular (*Synechococcus* sp. PCC 7942, hereinafter *Synechococcus*) cyanobacteria, and one unicellular green alga (*Chlamydomonas reinhardtii*, hereinafter *Chlamydomonas*) is reported.

The study of the antimicrobial mechanism of nanomaterials has been of great interest by the scientific community (Durán *et al.*, 2016; Franklin *et al.*, 2007; Rai *et al.*, 2009; Wyszogrodzka *et al.*, 2016). Most of the literature has established that the biocidal activities of metallic nanomaterials are due to the dissolved metal ions. In order to better understand the mechanism of action of these MOFs, three different approaches were used. Metal released from these MOFs and bioavailability of these metals were studied using ICP-MS, the chemical speciation program, Visual MINTEQ, and a heavy metal bioreporter bioanalytical tool, the cyanobacterium *Synechococcus elongatus* PPC7942 pBG2120 (hereinafter *Synechococcus* pBG2120) (Martin *et al.*, 2015). This bioreporter bears a fusion of the promoter region of the *smt* locus (encoding the transcriptional repressor SmtB and the metallothionein SmtA) to the *luxCDABE* operon of *Photobacterium luminescens* and is able to detect six different heavy metals (Zn, Ag, Cu, Co, Hg and Cd) in medium but also in environmental water samples.

To our knowledge, this work is the first study that reports the effects of these materials on photosynthetic organisms.

2. Materials and methods

2.1. Synthesis and characterization of materials

Zn-SIM1, Co-SIM1 and Ag-TAZ were synthesized by solvothermal procedure as reported elsewhere (Banerjee *et al.*, 2008; Farrusseng *et al.*, 2009; Huang *et al.*, 2006). All of them were characterized by X-ray diffraction (XRD) in order to assess their crystallinity. A brief description of each synthesis, the diffractogram and the scanning electron microscope (SEM) micrographs of crystals can be seen in Supplementary text S1 and Figs. S1 and S2.

2.2. Microorganism culture

In this study three different photosynthetic microorganisms were used, two different cyanobacterial

strains, one filamentous, *Anabaena* sp. PCC 7120 and one unicellular, *Synechococcus* sp. PCC 7942 and one unicellular green alga strain, *Chlamydomonas reinhardtii* Dangeard (strain CCAP 11/32A mt +). Each strain was grown in its specific medium. *Anabaena* cells were grown in AA/8 supplemented with nitrate (5 mM) (Allen and Arnon, 1955), *Synechococcus* in BG11 (Rippka, 1988) and *Chlamydomonas* in Tris-minimal phosphate medium (TAP-) (Hooper, 1989). All the media were adjusted to pH 7.5. The composition of these media are detailed in supplementary Table S1. All of them were grown on a rotatory shaker set under controlled conditions: 28 °C and 60 $\mu\text{mol photons m}^{-2} \text{s}^{-1}$ light intensity. For the free metal detection assays, a modified cyanobacterium based on *Synechococcus* sp. PCC 7942 was used, *Synechococcus elongatus* PBG2120, this strain was grown in BG11 medium supplemented with 3.2 $\mu\text{g mL}^{-1}$ of chloramphenicol (Cm) (Martin *et al.*, 2015).

2.3. Antimicrobial activity tests

2.3.1. Zone inhibition technique

The biocidal materials were subjected to an antimicrobial experiment using the diffusion method described by Fiebelkorn *et al.* (2003). Agar plate diffusion assay is the standardized method recommended by the National Committee for Clinical Laboratory standards, based on the method described by Bauer *et al.* (1966). Petri dishes were prepared with 20 mL of appropriate culture media plus 1% Agar. The cellular concentration in inocula was adjusted to $\text{OD}_{750\text{nm}} = 1$ for cyanobacteria and $\text{OD}_{750\text{nm}} = 0.5$ for the alga, using the corresponding culture medium. 500 μL of each microbial suspension were transferred to plates for inoculation, spread and allowed to dry at room temperature. The cells were allowed to grow during five days under 20 $\mu\text{mol photons m}^{-2} \text{s}^{-1}$ before the addition of the antimicrobials. All materials were used in powder form by placing 1 and 10 mg directly onto the inoculated agar plate. As a control of the toxicity exhibited by the ligands individually, 1 and 10 mg of each ligand were placed directly onto the inoculated agar plate at the same time. In all cases, the amount of ligand in these experiments was higher than that released by 1 or 10 mg of each MOF. Zone radius was measured from the outermost part of the MOF to the highest growth inhibition spot in the plates after 4, 24 and 48 h. Control plates were incubated at the same time without antimicrobial agents to check correct microbial growth.

2.3.2. MOFs suspensions bioassays

Microorganisms were exposed to 1 mg of each MOF in a final volume of 20 mL of each specific medium (50 mg L^{-1} final concentration). The procedure used was as follows: the three organisms were allowed to grow for five days, until they reached $\text{OD}_{750\text{nm}} = 1$ for cyanobacteria and $\text{OD}_{750\text{nm}} = 0.5$ for the alga. After the organisms reached the indicated OD, they were washed

tree times with each appropriate culture medium and 4 mL of each culture were added to 16 mL of culture media reaching $\text{OD}_{750\text{nm}} = 0.2$ for *Anabaena* and *Synechococcus* and $\text{OD}_{750\text{nm}} \text{OD} = 0.1$ for *Chlamydomonas*. MOFs were added fresh in each test. Before adding the microorganisms, 1 mg of each MOFs was weighed, added to the medium and in order to homogenize the MOFs in all the experiments, sonicated using a Ultrasonic bath (Ultrasons) during 1 min. Then, the organisms were grown on a rotatory shaker during the experiments time with the same conditions as described before. The initial cellular densities were selected in order to maintain all microorganisms in the exponential growth phase during the entire time of exposure (48 h). The pH was measured during the whole incubation period (up to 48 h). In the case of AA/8 + N (*Anabaena* medium), the mean pH during the whole experiment was 7.37 ± 0.02 , 7.35 ± 0.04 and 7.35 ± 0.05 for Ag-TAZ, Co-SIM1 and Zn-SIM1 exposure, respectively. In the case of BG11 (*Synechococcus* medium), the mean pH during the whole experiment was 7.37 ± 0.05 , 7.49 ± 0.05 and 7.43 ± 0.01 , for Ag-TAZ, Co-SIM1 and Zn-SIM1 exposure, respectively. For TAP- (*Chlamydomonas* medium), the pH evolution during the experiment time was 7.27 ± 0.03 , 7.29 ± 0.08 and 7.26 ± 0.03 for Ag-TAZ, Co-SIM1 and Zn-SIM1 exposure, respectively. Microbial growth as measured by increase in $\text{OD}_{750\text{nm}}$ could not be used due to potential attachment of MOFs to the microorganisms, for that, chlorophyll *a* concentration was used as endpoint as described for diatoms (Bazes *et al.*, 2009; Briand, 2009; Tsoukatou *et al.*, 2002). As a control of the toxicity exhibited by the ligands individually, the microorganisms were exposed at the same time to 50 mg L^{-1} of each ligand. The amount of the total ligand available from 50 mg L^{-1} of each MOF was 38.75 mg L^{-1} and 39.75 mg L^{-1} of SIM1 ligand for Zn-SIM1 and Co-SIM1, respectively, and 19.6 mg L^{-1} of TAZ ligand for Ag-TAZ. Thus, in all cases, the amount of ligand in these experiments was higher than that released by 50 mg L^{-1} of each MOF. Specifically, 50 mg L^{-1} of SIM-1 ligand (Co-SIM1 and Zn-SIM1 ligand) correspond to 1.25 and 1.3 fold more ligand than that released by 50 mg L^{-1} of Co-SIM1 and Zn-SIM1, respectively. In the case of TAZ ligand (Ag-TAZ ligand), the amount of TAZ is 2.5 times higher than that available in the release of 50 mg L^{-1} of Ag-TAZ.

In addition, the biocidal activity of the pure metal salts was also studied. The three microorganisms were exposed to the equivalent metal ion concentration presented in 50 mg L^{-1} of each MOF, specifically, 11.5 mg L^{-1} of Zn^{2+} [52.32 mg L^{-1} of $\text{Zn}(\text{NO}_3)_2 \cdot 6\text{H}_2\text{O}$], 10.65 mg L^{-1} of Co^{2+} [52.5 mg L^{-1} of $\text{Co}(\text{NO}_3)_2 \cdot 6\text{H}_2\text{O}$] and 30.68 mg L^{-1} of Ag^+ (48 mg L^{-1} of AgNO_3). After 4, 24 and 48 h, chlorophyll was extracted from 1 mL of each experiment in methanol at 4 °C for 24 h in darkness and the chlorophyll *a* concentration of the cyanobacteria estimated according

to Marker (1972) and in a 90% acetone aqueous solution for the alga according to Jeffrey and Humphrey (1975). The absorbance was determined by measuring the extract using a HITACHI U-2000 spectrophotometer at appropriate wavelengths. Two replicates of 1 mL were used and the experiments were performed in triplicate. The data are expressed as the percentage of the chlorophyll *a* concentration of the treated samples in function of the chlorophyll *a* concentration of the untreated samples.

2.3.3. MOFs filtrate bioassays

In order to analyze which part of the MOFs toxicity was due to the dissolved metals released from the MOFs, MOFs filtrate experiments were performed as follows: 1 mg of each MOF was weighed, added to 20 mL of each medium and sonicated during 1 min. MOF sonicated suspensions were kept for 24 h and centrifuged (4500 g 15 min) in 50 kDa molar mass cut-off VIVASPIN ultrafiltration membranes (Sartorius) for separating the ion released from the MOFs. 16 mL of the filtrate were used as the experimental medium. The organisms were prepared as in the Section 2.3.2. (see above) and the chlorophyll *a* concentration was measured after 24 h in the same way as described before. Each media without MOFs were also centrifuged and used as controls.

2.4. Detection of dissolved metals from MOFs by ICP-MS

The concentration of the dissolved metals present in MOFs filtrates in each medium (see above), and also, the concentration of the dissolved metals released from MOFs (50 mg L⁻¹) in distilled water was measured by inductively coupled plasma-mass spectrometry (ICP-MS; Perkin-Elmer Sciex Elan 6000 equipped with an AS91 auto-samples), by the ICP-MS laboratory of the Universidad Autónoma de Madrid, after removing the solids by 50 kDa VIVASPIN ultrafiltration membranes (Sartorius) after 4, 24 and 48 h of exposure.

2.5. Detection of the dissolved metals from MOFs by a heavy metal bioreporter

The bioluminescence strain, *Synechococcus* pBG2120, was prepared as described previously (Martin *et al.*, 2015). Briefly, 50 mg L⁻¹ of each MOF in distilled water were centrifuged in 50 kDa VIVASPIN ultrafiltration membranes after 24 h and the concentration of the dissolved metal present in these filtrates measured by ICP-MS (see above). The filtrates collected were diluted several times and 300 µL of these dilutions were added to 1200 µL of the bioreporter culture in 24 well plates. The plates were incubated at 28 °C in light (60 µmol m⁻² s⁻¹) on a rotatory shaker up to 4 h. For the luminescence measurements, 100 µL of cell suspensions were transferred to an opaque 96-well microtiter plate and luminescence was recorded every 5 min for 20 min in a CentroLB960 luminometer (Berthold Technologies GmbH and Co. KG, Bald Wilbad, Germany).

2.6. Modeling of metal speciation

The chemical equilibrium model Visual MINTEQ was used to predict the metal speciation in the three growth media, BG11, AA/8 + N and TAP-. Assumptions of a fixed pH, fixed potential redox (Eh), closed system and no precipitation of solid phases were made during computations. This chemical model was used previously to predict metal speciation and link it to the response of the reporter strain *Synechococcus* pBG2120 (Martin *et al.*, 2015).

2.7. Modeling of metal speciation

The test of statistically significant differences between datasets was performed using One-Way Analyses of Variance (ANOVA); also, to discriminate which datasets were significantly different from the others, the *post-hoc* Tukey's HSD (honestly significant difference) test was performed. All the tests were computed using R software 3.0.2. (The Foundation for Statistical Computing).

3. Results and discussion

3.1. Antimicrobial activity tests

3.1.1. Inhibition zone testing bioassay

The three organisms were exposed to 1 and 10 mg of each MOF up to 48 h. When exposed to 1 mg, both cyanobacteria were more sensitive to Co-SIM, presenting an inhibition radius of around 3 mm for *Synechococcus* and 5 mm for *Anabaena*. In the case of *Synechococcus*, Zn-SIM1 and Ag-TAZ produced an inhibition radius of 2 and 1 mm, respectively. *Anabaena* exhibited an inhibition radius of 1 mm and 3 mm for Zn-SIM1 and Ag-TAZ, respectively, after 24 h. In the case of *Chlamydomonas*, none of the MOFs caused any inhibition after 24 h of exposure (Fig. 1), and, after 48 h, only the MOF based on Ag, Ag-TAZ, caused an inhibition radius of 4 mm to this alga (not shown).

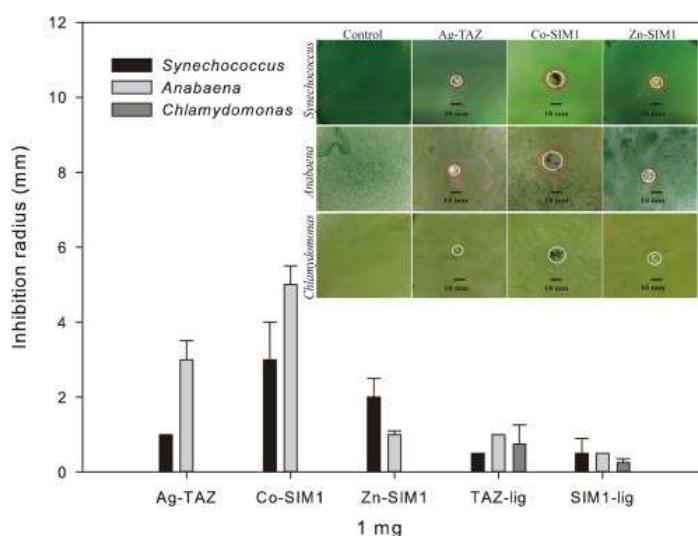


Figure 1. Zone inhibition technique experiment to estimate antimicrobial activity towards *Synechococcus*, *Anabaena* and *Chlamydomonas* after exposure to 1 mg of Ag-TAZ, Co-

SIM1 and Zn-SIM1 MOFs and TAZ-lig and SIM1-lig (ligands) for 24 h. Inhibition radii (mm) and photos of the agar plates showing the inhibition zones are included. The white circles indicate deposited material and the red circles indicate inhibition zones. (For interpretation of the references to color in this figure legend, the reader is referred to the web version of this article.)

When organisms were exposed to 10 mg of each MOF, also Co-SIM1 was the most toxic MOF for both cyanobacteria, *Synechococcus* and *Anabaena*, causing 8 and 6 mm of inhibition radius after 24 h of exposure, respectively. Again, Ag-TAZ was the only MOF that caused growth inhibition to *Chlamydomonas*, around 5 mm of inhibition radius after 24 h of exposure (Fig. S3). Exposure to 1 or 10 mg of ligands did not exceed 1 mm or 2 mm of inhibition radius respectively.

As previously reported by Aguado *et al.* (2014) Co-SIM1 showed a significant antimicrobial activity. They found that Co-SIM exhibited higher biocidal activity towards *S. cerevisiae*, *P. putida* and *E. coli* than Ag-TAZ, however, although a high biocidal effect towards both cyanobacteria was found, the results showed that it was not effective towards the green alga *Chlamydomonas* at the concentration tested. Other authors (Refat *et al.*, 2008; Wojciechowska *et al.*, 2012) have investigated the biological activities of Zn based complexes, specifically, in the case of L-tyrosinate Zinc(II) complex, Refat *et al.* (2008) found moderate activity of this complex against *E. coli* but strong activity against *Bacillus subtilis*, *Serratia* and *Pseudomonas aeruginosa*. Wojciechowska *et al.* (2012) incorporated ligand modifications to these L-tyrosinate complexes, as a molecule of secondary ligand such as 2,2'-bipyridine or imidazole. They found that only the complexes based on imidazole ligands presented large antibacterial activity, suggesting that the biocidal activity was strongly correlated with the presence of the imidazole molecule in its structure. However, the results reported in this study did not show toxicity of the imidazole, suggesting that the biocidal activity of Zn-SIM1 and Co-SIM1 against the cyanobacteria might be due to the dissolved metal. The biocidal effects of Ag based MOFs are well-documented, Lu *et al.* (2014) showed that two silver carboxylate MOFs, $[\text{Ag}_2(\text{O-IPA})(\text{H}_2\text{O}) \cdot (\text{H}_3\text{O})]$ and $\text{Ag}_5(\text{PYDC})_2(\text{OH})$ exhibited excellent antibacterial activities towards *E. coli* and *S. aureus*. Berchel *et al.* (2011) presented a silver MOF material based on a 3-phosphonobenzoate ligand which placing 1 mg onto an agar plate resulted in a strong growth inhibition upon six different strains of *S. aureus*, *E. coli* and *P. aeruginosa*. All these previous studies studied the antimicrobial properties of these materials on heterotrophic organisms. Our experiments showed that all MOFs used were able to diffuse in the cyanobacterial media and inhibit their growth. However, only the Ag-TAZ was able to inhibit the growth of the alga at the tested concentration. The inhibition zone in each plate remained at least three

months so that the biocidal activity was kept over time (not shown).

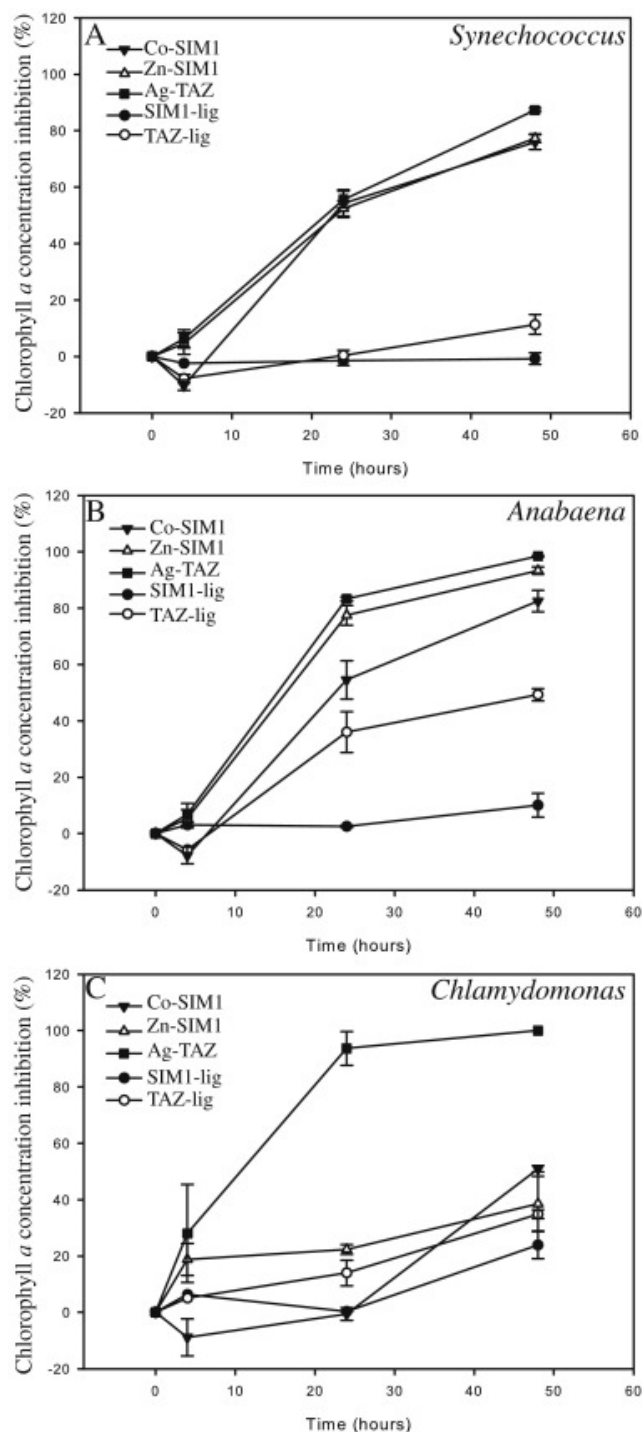


Figure 2. Chlorophyll a concentration inhibition caused by exposure to Ag-TAZ, Co-SIM1 and Zn-SIM1 MOFs and TAZ-lig and SIM1-lig (ligands) of (A) *Synechococcus*, (B) *Anabaena* and (C) *Chlamydomonas* to 50 mg L⁻¹. Data represent the mean ± standard deviation of at least three independent experiments.

3.1.2. MOF suspension bioassays

To further study the mechanism of action of these MOFs, we also performed tests to determine the biocidal effect of the tested materials in suspension. The three microorganisms were exposed to 50 mg L⁻¹ of each MOF. As controls, the microorganisms were also exposed to 50 mg L⁻¹ of each organic ligand and to the equivalent metal ion concentration presented in 50

mg L⁻¹ of each MOF as metal salts (see Materials and Methods). Chlorophyll a concentration was measured after 4, 24 and 48 h of exposure. All the experiments were performed in the culture medium specific for each organism (Table S1) and with the organisms in their exponential growth phase. Fig. 2 shows the results of these experiments.

As observed in Fig. 2A, for *Synechococcus* all MOFs caused around 50% of chlorophyll a concentration inhibition after 24 h of exposure. After 48 h of exposure, both Co-SIM1 and Zn-SIM1, reached 80% of chlorophyll a concentration inhibition and Ag-TAZ was slightly more toxic, exceeding 85% of inhibition.

Anabaena was more sensitive to Ag-TAZ and Zn-SIM1, exposure to these MOFs resulted in around 80% of chlorophyll a concentration inhibition after 24 h of exposure. In the case of Co-SIM1, it provoked 50% of chlorophyll a concentration inhibition after 24 h and near 80% of inhibition after 48 h of exposure (Fig. 2B). Unlike the results observed according to the inhibition zone testing, in liquid media all MOFs caused

practically the same degree of inhibition towards both cyanobacteria. In fact, in the case of *Anabaena*, toxicity caused by Ag-TAZ and Zn-SIM1 was higher than that caused by Co-SIM1. These results showed an increased biocidal activity in liquid media vs. agar plate suggesting an increase in the release of dissolved metals or an increase in the cell contact with these materials. This fact has a very important implication when these materials are designed to be in contact with aqueous media. *Chlamydomonas* presented high sensitivity to Ag-TAZ, causing 90% of chlorophyll a concentration inhibition after 24 h of exposure, as observed by the inhibition zone method (Fig. 1 and Fig. S1). However, Co-SIM1 and Zn-SIM1 were much less toxic, causing 40 and 30% of inhibition after 48 h, respectively, (Fig. 2C). As observed above, in general, both ligands did not show a significant toxicity, only TAZ ligand towards *Anabaena*, (Fig. 2B), showed a significant inhibition of 35%. However, this concentration of ligand was 2.5 fold higher than that released by 50 mg L⁻¹ of Ag-TAZ (see Materials and Methods); implying that the ligand actually released from the MOFs was not relevant for toxicity.

Regarding the activity of pure metal salts, in all cases, we obtained a highest antimicrobial action of the metal salts compared to the biocidal action exhibited by the MOFs, which can be attributed to the immediate bioavailability of these metal ions (Fig. S4).

3.1.3. MOFs filtrate bioassays

Most of the literature has established that the biocidal activities of metallic nanomaterials are due to the dissolved metal ions (Aruoja *et al.*, 2009; Li *et al.*, 2015; Navarro *et al.*, 2008; Wyszogrodzka *et al.*, 2016), however, in some cases, direct contact between the organism and the material could be also responsible of the observed toxicity (Rodea-Palomares *et al.*,

2011; Zhuang *et al.*, 2012). To determine the contribution of dissolved metals to MOFs toxicity, MOF filtrates experiments were performed. The dissolved metal present in each MOF filtrate was designed as Co_d, Zn_d or Ag_d.

First of all, the dissolved metal concentration released from these three different MOFs in distilled water and in each culture medium along time was measured by ICP-MS (Fig. 3). In all cases, a rapid increase of the metal concentration was observed during the first hours, probably due to the release of surface metals, which occurs first. Then, the metal concentration linearly increased within 48 h. In general, all MOFs showed similar quantity of metal released in the different media (Fig. 3), being Co-SIM1 which released more quantity of metal, achieving concentrations of 10, 8 and 12 mg L⁻¹ of Co_d in AA/8+N, BG11 and TAP- after 24 h, respectively. However, it is remarkable that Co-SIM1 released lesser quantity of cobalt in distilled water than in the other media (Fig. 3). Zn-SIM1 released around 2 mg L⁻¹ of Zn_d in all media after 24 h; Ag-TAZ was by far the MOF which released less metal amount, reaching 0.0128, 0.1896 and 0.3158 mg L⁻¹ of Ag_d in AA/8 + N, BG11 and TAP- after 24 h, respectively.

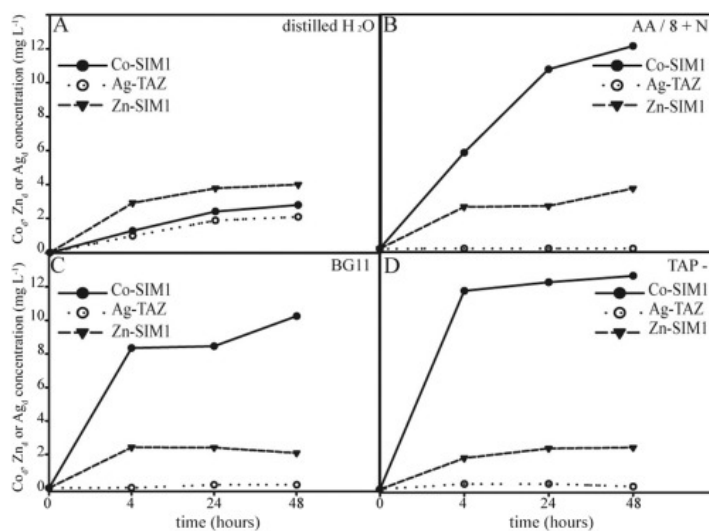


Figure 3. Time evolution of dissolved metal (Co_d, Ag_d, Zn_d) released from Co-SIM1, Ag-TAZ and Zn-SIM1 MOFs, respectively in (A) distilled water, (B) AA/8 + N, (C) BG11 and (D) TAP- (MOF initial concentration 50 mg L⁻¹).

As shown in Fig. 4, dissolved metals can explain the biocidal activity of the tested MOFs. There were no significant differences for the three organisms when performing MOF suspensions (MOF_s) bioassays or when using MOF filtrates (MOF_f), except for Ag-TAZ. Regarding *Synechococcus*, Ag-TAZ filtrate (Ag-TAZ_f) caused significantly ($p < 0.05$) more toxicity than the toxicity exhibited by Ag-TAZ suspensions (Ag-TAZ_s). However, in the case of *Anabaena* and *Chlamydomonas*, Ag-TAZ_s was significantly ($p < 0.001$ and $p < 0.01$, respectively) more toxic than Ag-TAZ_f. These differences may be due to slight differences in dissolved metals released from MOFs in

the presence of the organisms as has been reported before (Aguado *et al.*, 2014; Navarro *et al.*, 2008).

All together the results present evidences that the toxicity of these MOFs is strongly mediated by the dissolved metals leaked from them. These results are consistent with other studies (Aguado *et al.*, 2014; Berchel *et al.*, 2011; Lu *et al.*, 2014). These authors found that these MOFs could act as a reservoir of ions and the slow release of these metal ions leads to an excellent and long-term microbial activity. In order to elucidate how long the different MOFs might be releasing these metals, we calculated the release rate in distilled water. The initial time point of the experiment was not included in the calculations to disregard the initial surface metal released from the MOFs. In the case of Co-SIM1, the rate of Co_d release was equal to $0.68 \pm 0.20 \text{ mg Co}_d \text{ g MOF}^{-1} \text{ h}^{-1}$. Zn-SIM1 and Ag-TAZ, presented a metal release rate of $0.48 \pm 0.17 \text{ mg Zn}_d \text{ g MOF}^{-1} \text{ h}^{-1}$ and $0.50 \pm 0.18 \text{ mg Ag}_d \text{ g MOF}^{-1}$

h^{-1} , respectively. Taking into account the total metal concentration present in the different MOFs, the Co_d release would remain 314 h, 1235 h in the case of Ag_d release from Ag-TAZ and 482 h for Zn_d released from Zn-SIM1. This can ensure the biocidal capacity of the MOFs over time as observed in the inhibition zone testing bioassays.

As reported by other authors (Lu *et al.*, 2014; Ruyra *et al.*, 2015), there is a correlation between the structure and the biocidal activity of the MOFs. The different frameworks may have discriminating capacities to release metal ions, which lead to differences between their biocidal activities. In addition, those that released sufficiently high amounts of soluble metal ions known to be moderately or highly toxic in their free form will exhibit a greater biocidal capacity. While, those MOFs that release significant amounts of soluble metal ions, but whose constituent metal ion is not toxic in the free form will show little or no biocidal capacity. However,

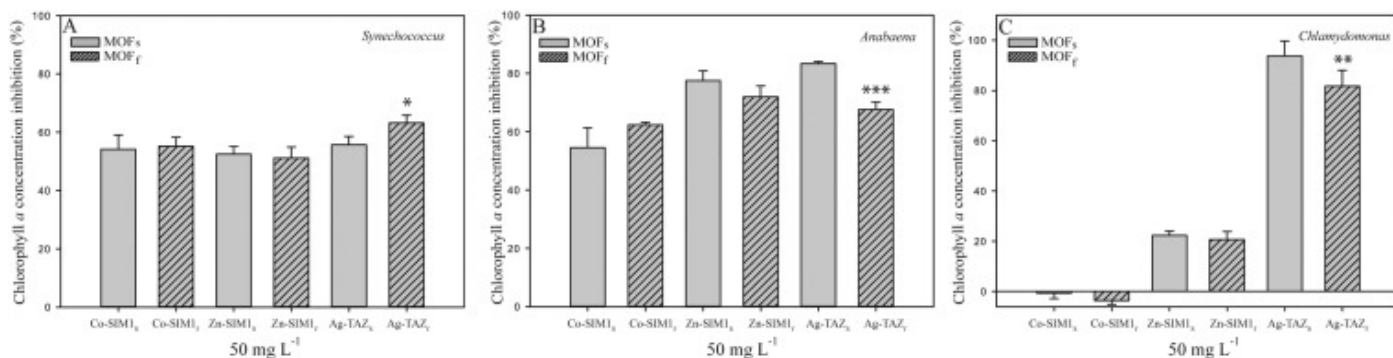


Figure 4. Chlorophyll *a* concentration inhibition of (A) *Synechococcus*, (B) *Anabaena* and (C) *Chlamydomonas* exposed to 50 mg L^{-1} of Co-SIM1, Zn-SIM1 and Ag-TAZ MOFs. Comparison between MOFs suspensions (MOFs) and MOFs filtrates (MOF_f) bioassays are shown. Statistically differences are indicated by “*” = $p < 0.05$, “***” = $p < 0.01$ and “****” = $p < 0.001$. Data represent the mean \pm standard deviation of at least three independent experiments.

the biocidal capacity may also be influenced by the speciation of these metals in the different media and the sensitivity of the microorganism tested. Although these previous studies have related the toxicity with the dissolved ions, speciation of these dissolved metals in the different media used for the toxicity assays were not performed.

As metal speciation is a relevant issue determining the availability and therefore the toxicity of metals (Campbell, 1995; Campbell *et al.*, 2002; Paquin *et al.*, 2002), the chemical speciation program, Visual MINTEQ, was used in order to elucidate if these differences between organisms’ sensitivity to the different MOFs are due to differences in bioavailability of the dissolved metals released from these MOFs in the different media. In Table S2, the percentages of the main species predicted by Visual MINTEQ for the dissolved metals released from 50 mg L^{-1} of MOFs in each medium after 24 h are shown.

As can be seen, each medium presented different percentages of free ion, which has been described as the main bioavailable specie according to the Free Ion

Model (FIM) (Campbell *et al.*, 2002). In accordance with the speciation modeling, the Co^{2+} available is significantly higher than the other ions due to the high release capacity of this MOF in the media and to the high predicted Co^{2+} percentage in all media. The percentage of Zn and Co free ion in the green alga medium (TAP-) was slightly higher than in the other media. However, only 2% of the total Ag dissolved in this medium was presented as Ag^+ in comparison with 57% and 49% presented in BG11 and AA/8 + N, respectively.

As detailed before, at the same concentration tested, both cyanobacteria presented over 50% of chlorophyll *a* concentration inhibition for the three MOFs after 24 h of exposure, however, the green alga only showed a clear sensitivity to Ag-TAZ, reaching 90% of chlorophyll *a* concentration inhibition after 24 h. In order to explain the different sensitivity shown by the three microorganisms, it has to be considered, as previously described for *Chlamydomonas*, that for this alga silver internalization is very rapid (Fortin and Campbell, 2000; Lee *et al.*, 2005). On the other hand, Macfie *et al.* (1994) and Macfie and Welbourn

(2000) studied the effect of the cell wall of *Chlamydomonas* as a barrier towards heavy metals uptake such as Cd, Co, Cu and Ni. They concluded that the algal cell wall offered some protection from potentially toxic concentrations of certain metals, in the case of Co^{2+} , this tolerance appeared to be related to the binding of this metal to the cell wall (Macfie and Welbourn, 2000), although the protection varied with each metal and was limited to a specific range of concentration. Therefore, if Zn and Co-MOFs concentrations exposed towards the alga were increased (Fig. 5), cell wall might no longer have a protective effect leading to the occurrence of toxicity. As can be seen in Fig. 5, at 200 mg L^{-1} , Zn-MOF cause 20% of inhibition and Co-SIM 40% after 24 h of exposure while after 48 h, both MOFs caused nearly 80% of chlorophyll *a* concentration inhibition. As highlighted by other authors (Li *et al.*, 2015), it is very important to take into account the diversity in cell wall composition or surface architecture in studies of algal interaction with nanomaterials.

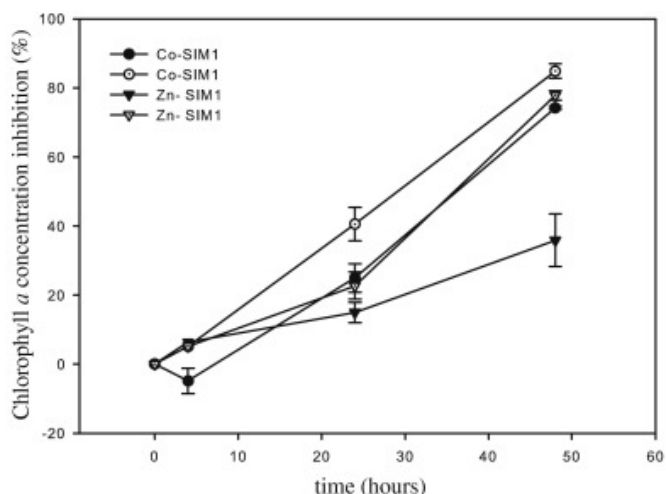


Figure 5. Time evolution of dissolved metal (Co_d , Ag_d , Zn_d) released from Co-SIM1, Ag-TAZ and Zn-SIM1 MOFs, respectively in (A) distilled water, (B) AA/8 + N, (C) BG11 and (D) TAP- (MOF initial concentration 50 mg L^{-1}).

Summarizing, Ag-TAZ was the most toxic MOF for the three microorganisms with a metal ion released rate slower than Co-SIM1, which showed the highest ion released rate.

3.2. Heavy metal bioreporter detection assays

In order to complete the information about the bioavailability of the dissolved metals released from these MOFs, a new approach using a heavy metal whole-cell bioreporter was implemented. In contrast to chemical methods, heavy metals whole-cell bioreporters measure the bioavailable metal, which is the fraction that interacts with the cell and consequently is detected by the organisms. Usually, this fraction corresponds to the free ion specie, capable of passing through cellular membranes. For that, bioavailability of the dissolved metals (Ag_d , Zn_d and Co_d) released from MOFs was compared between the free ion

concentration predicted by Visual MINTEQ and a heavy metal bioreporter based on a cyanobacterium, *Synechococcus elongatus* pBG2120. As shown in Table 1, in the case of Ag_d and Co_d the concentration detected by the bioreporter was very close to the free ion concentration predicted by Visual MINTEQ program. However, regarding Zn_d , the concentration detected by the bioreporter was much higher than the free ion concentration predicted by the program. One plausible explanation of that, as reported by other authors, is the uptake of a metal-ligand complex across the biological membrane (Krom *et al.*, 2000; Zhao *et al.*, 2016). Besides, Errecalde *et al.* (1998) have elucidated that the toxicity of Cd^{2+} and Zn^{2+} is enhanced in the presence of citrate against the green alga, *Pseudokirchneriella subcapitata*. They have concluded that the bioavailability of divalent metals in the presence of citrate may well diverge from the predictions of the Free ion model (FIM). As can be seen in Table S2, in the bioreporter medium assay (BG11) the 54% of the total Zn_d appeared as Zn-citrate complex, which could be increasing the concentration of Zn detecting by the bioreporter.

Table 1. Comparison between free ion predicted concentration by Visual MINTEQ and the bioreporter output.

Metal dissolved	Free-ion predicted by Visual MINTEQ (mg L^{-1})	Bioreporter output (mg L^{-1})
Zn_d	0.007	N.D.
	0.015	N.D.
	0.029	0.132 ± 0.012
	0.058	0.209 ± 0.120
	0.117	0.446 ± 0.033
Ag_d	0.007	N.D.
	0.014	0.020 ± 0.001
	0.028	0.027 ± 0.013
	0.056	0.042 ± 0.010
	0.112	N.D.
Co_d	0.014	N.D.
	0.028	N.D.
	0.056	0.068 ± 0.005
	0.112	0.112 ± 0.005
	0.224	0.188 ± 0.001

N.D. Not detected.

We can conclude that the free ion metal is most likely the species available and detected by photosynthetic microorganisms and it is probably the chemical species responsible of the toxicity shown by these MOFs although some metal-complexes could interact with these organisms as well.

4. Conclusions

In summary, these Co, Zn and Ag-MOFs presented high antimicrobial activity towards photosynthetic

organisms such as cyanobacteria or algae after a very short time of exposure. These characteristics make these materials suitable for use as antimicrobial materials against biofouling process, specifically, “slime” constitution.

Also, a combined analytical chemistry, chemical modeling and bioanalytical strategy was used to better understand the antibiofouling properties of these materials. Based on these different approaches we have elucidated that the biocidal activity presented by these MOFs was due to the dissolved metals released from them and more exactly, it depended on the bioavailability presented by these metal ions, which was closely related with the free ion concentration.

Bioavailability and toxicity of the free ions as well as the release rate of these ions from the MOFs determine the biocidal capacity of each MOF. Thus, due to the slower release rate of Ag⁺ from Ag-TAZ and the toxic capacity of this metal ion, Ag-TAZ presents the best characteristics for practical applications. However, taking into account the metal release capacity of the different MOFs and the sensitivity of the target microorganisms, MOFs based on other metals such as Co and Zn can be also designed and used as biocides. The different sensitivities between species have to be taken into account, especially, if these materials are designed to prevent colonization of surfaces by different organisms. Furthermore, the gradual release of the metal ions would provide a sustained long-term biocidal activity towards photosynthetic organisms.

Acknowledgements

This research was supported by the Spanish Ministry of Economy, CTM2013-45775-C2-1-R and CTM2013-45775-C2-2-R.

References

- Aguado, S., Canivet, J., Farrusseng, D., 2010. Facile shaping of an imidazolate-based MOF on ceramic beads for adsorption and catalytic applications. *Chem. Commun.*, 46, 7999–8001.
- Aguado, S., Canivet, J., Farrusseng, D., 2011. Engineering structured MOF at nano and macroscales for catalysis and separation. *J. Mater. Chem.*, 21, 7582–7588.
- Aguado, S., Quiros, J., Canivet, J., Farrusseng, D., Boltes, K., Rosal, R., 2014. Antimicrobial activity of cobalt imidazolate metal-organic frameworks. *Chemosphere*, 113, 188–192.
- Allen, M.B., Arnon, D.I., 1955. Studies on Nitrogen-fixing blue-green algae. I. Growth and nitrogen fixation by *Anabaena cylindrica*. *Lemm. Plant Physiol.*, 30, 366–372.
- Aruoja, V., Dubourguier, H.C., Kasemets, K., Kahru, A., 2009. Toxicity of nanoparticles of CuO, ZnO and TiO₂ to microalgae *Pseudokirchneriella subcapitata*. *Sci. Total Environ.*, 407, 1461–1468.
- Banerjee, R., Phan, A., Wang, B., Knobler, C., Furukawa, H., O’Keeffe, M., Yaghi, O.M., 2008. High-throughput synthesis of zeolitic imidazolate frameworks and application to CO₂ Capture. *Sci.*, 319, 939–943.
- Banerjee, R., Furukawa, H., Britt, D., Knobler, C., O’Keeffe, M., Yaghi, O.M., 2009. Control of pore size and functionality in isoreticular zeolitic imidazolate frameworks and their carbon dioxide selective capture properties. *J Am Chem Soc.*, 131, 3875–3877.
- Bauer, A.W., Kirby, W.M., Sherris, J.C., Turck, M., 1966. Antibiotic susceptibility testing by a standardized single disk method. *Am. J. Clin. Pathol.*, 45, 493–496.
- Bazes, A., Silkina, A., Douzenel, P., Fay, F., Kervarec, N., Morin, D., Berge, J.P., Bourgougnon, N., 2009. Investigation of the antifouling constituents from the brown alga *Sargassum muticum* (Yendo) Fensholt. *J. Appl. Phycol.*, 21, 395–403.
- Beg, S., Rahman, M., Jain, A., Saini, S., Midoux, P., Pichon, C., Ahmad, F.J., Akhter, S., 2016. Nanoporous metal organic frameworks as hybrid polymer-metal composites for drug delivery and biomedical applications. *Drug Discov Today.*, in press, doi: 10.1016/j.drudis.2016.10.001.
- Berchel, M., Gall, T.L., Denis, C., Hir, S.L., Quentel, F., Elléouet, C., Montier, T., Rueff, J.M., Salaün, J.Y., Haelters, J.P., Hix, G.B., Lehn, P., Jaffrès, P.A., 2011. A silver-based metal–organic framework material as a ‘reservoir’ of bactericidal metal ions. *New J. Chem.*, 35, 1000–1003.
- Blaser, S.A., Scheringer, M., Macleod, M., Hungerbühler, K., 2008. Estimation of cumulative aquatic exposure and risk due to silver: contribution of nano-functionalized plastics and textiles. *Sci. Total Environ.*, 390, 396–409.
- Briand, J.F., 2009. Marine antifouling laboratory bioassays: an overview of their diversity. *Biofouling*, 25, 297–311.
- Campbell, P.C. 1995. Interactions between trace metals and aquatic organisms: a critique of the free-ion activity model. In: A. Tessier and D.R. Turner, eds, *Metal speciation and bioavailability in aquatic systems*, 3, 45–102.
- Campbell, P.G., Errecalde, O., Fortin, C., Hiriart-Baer, V.P., Vigneault, B., 2002. Metal bioavailability to phytoplankton--applicability of the biotic ligand model. *Comp. Biochem. Physiol. C Toxicol. Pharmacol.*, 133, 189–206.
- Dang, H., Lovell, C.R., 2016. Microbial surface colonization and biofilm development in marine environments. *Microbiol. Mol. Biol. Rev.*, 80, 91–138.
- Díez, B., Roldán, N., Martín, A., Sotto, A., Perdígón-Melón, J.A., Arsuaga, J., Rosal, R., 2017. Fouling and biofouling resistance of metal-doped

- mesostructured silica/polyethersulfone ultrafiltration membranes. *J. Membr. Sci.*, 526, 252–263, 2017.
- Dong, B., Belkhair, S., Zaarour, M., Fisher, L., Verran, J., Tosheva, L., Retoux, R., Gilson, J.P., Mintova, S., 2014. Silver confined within zeolite EMT nanoparticles: Preparation and antibacterial properties. *Nanoscale*, 6, 10859–10864.
- Durán, N., Durán, M., de Jesus, M.B., Seabra, A.B., Fávoro, W.J., Nakazato, G., 2016. Silver nanoparticles: A new view on mechanistic aspects on antimicrobial activity. *Nanomedicine: Nanotech. Biol. Med.*, 12, 789–799.
- Egger, S., Lehmann, R.P., Height, M.J., Loessner, M.J., Schuppler, M., 2009. Antimicrobial properties of a novel silver-silica nanocomposite material. *Appl. Environ. Microbiol.*, 75, 2973–2976.
- Errecalde, O., Seidl, M., Campbell, P.G.C., 1998. Influence of a low molecular weight metabolite (citrate) on the toxicity of cadmium and zinc to the unicellular green alga *Selenastrum Capricornutum*: An exception to the free-ion model. *Water Res.*, 32, 419–429.
- Farrusseng, D., Aguado, S., Canivet, J., 2009. Zeolitic organic-inorganic functionalised imidazolate material, method for preparing same and uses thereof. *Eur. Pat. WO.*, 2011033233.
- Ferey, G., 2008. Hybrid porous solids: Past, present, future. *Chem. Soc. Rev.*, 37, 191–214.
- Fiebelkorn, K.R., Crawford, S.A., McElmeel, M.L., Jorgensen, J.H., 2003. Practical disk diffusion method for detection of inducible clindamycin resistance in *Staphylococcus aureus* and coagulase-negative *Staphylococci*. *J. Clin. Microbiol.*, 41, 4740–4744.
- Fortin, C., Campbell, P.G.C., 2000. Silver uptake by the green alga *Chlamydomonas reinhardtii* in relation to chemical speciation: Influence of chloride. *Environ. Toxicol. Chem.*, 19, 2769–2778.
- Franklin, N.M., Rogers, N.J., Apte, S.C., Batley, G.E., Gadd, G.E., Casey, P.S., 2007. Comparative toxicity of nanoparticulate ZnO, bulk ZnO, and ZnCl₂ to a freshwater microalga (*Pseudokirchneriella subcapitata*): The importance of particle solubility. *Environ. Sci. Technol.*, 41, 8484–8490.
- Furukawa, H., Cordova, K.E., O'Keeffe, M., Yaghi, O.M., 2013. The chemistry and applications of metal-organic frameworks. *Science*, 341, 1230444.
- Getman, R.B., Bae, Y.S., Wilmer, C.E., Snurr, R.Q., 2012. Review and analysis of molecular simulations of methane, hydrogen, and acetylene storage in metal-organic frameworks. *Chem Rev.*, 112, 703–723.
- Haasnoot, J.G., 2000. Mononuclear, oligonuclear and polynuclear metal coordination compounds with 1,2,4-triazole derivatives as ligands. *Coord. Chem. Rev.*, 200–202, 131–185.
- Hooper, J.K., 1989. The *Chlamydomonas* Sourcebook. A Comprehensive Guide to Biology and Laboratory Use. Academic Press, San Diego, 1989.
- Horcajada, P., Chalati, T., Serre, C., Gillet, B., Sebrie, C., Baati, T., Eubank, J.F., Heurtaux, D., Clayette, P., Kreuz, C., Chang, J.S., Hwang, Y.K., Marsaud, V., Bories, P.N., Cynober, L., Gil, S., Férey, G., Couvreur, P., Gref, R., 2010. Porous metal-organic-framework nanoscale carriers as a potential platform for drug delivery and imaging. *Nat. Mater.*, 9, 172–178.
- Huang, X.C., Lin, Y.Y., Zhang, J.P., Chen, X.M., 2006. Ligand-directed strategy for zeolite-type metal-organic frameworks: zinc(II) imidazolates with unusual zeolitic topologies. *Angew. Chem. Int. Ed.*, 45, 1557–1559.
- Jeffrey, S.W., Humphrey, G.F., 1975. New spectrophotometric equations for determining chlorophylls a, b, c1 and c2 in higher plants, algae and natural phytoplankton. *Biochem. Physiol. Pflanzen*, 167, 191–194.
- Kim, Y.H., Lee, D.K., Cha, H.G., Kim, C.W., Kang, Y.C., Kang, Y.S., 2006. Preparation and characterization of the antibacterial Cu nanoparticle formed on the surface of SiO₂ nanoparticles. *J. Phys. Chem.*, 110, 24923–24928.
- Kreno, L.E., Leong, K., Farha, O.K., Allendorf, M., Van Duyne, R.P., Hupp, J.T., 2012. Metal-organic framework materials as chemical sensors. *Chem Rev.* 112, 1105–1125.
- Krom, B.P., Warner, J.B., Konings, W.N., Lolkema, J.S., 2000. Complementary metal ion specificity of the metal-citrate transporters CitM and CitH of *Bacillus subtilis*. *J. Bacteriol.* 182, 6374–6381.
- Kuppler, R.J., Timmons, D.J., Fang, Q.R., Li, J.R., Makal, T.A., Young, M.D., Yuan, D., Zhao, D., Zhuang, W., Zhou, H.C., 2009. Potential applications of metal-organic frameworks. *Coord. Chem. Rev.*, 253, 3042–3066.
- Lalueza, P., Monzón, M., Arruebo, M., Santamaría, J., 2011. Bactericidal effects of different silver-containing materials. *Mater. Res. Bull.*, 46, 2070–2076.
- Lee, D.Y., Fortin, C., Campbell, P.G., 2005. Contrasting effects of chloride on the toxicity of silver to two green algae, *Pseudokirchneriella subcapitata* and *Chlamydomonas reinhardtii*. *Aquat Toxicol.* 75, 127–135.
- Lemire, J.A., Harrison, J.J., Turner, R.J., 2013. Antimicrobial activity of metals: Mechanisms, molecular targets and applications. *Nat. Rev. Microbiol.*, 11, 371–384.
- Li, X., Schirmer, K., Bernard, L., Sigg, L., Pillai, S., Behra, R., 2015. Silver nanoparticle toxicity and association with the alga *Euglena gracilis*. *Environ. Sci. Nano*, 2, 594–602.

- Liu, Y., Xu, X., Xia, Q., Yuan, G., He, Q., Cui, Y., 2010. Multiple topological isomerism of three-connected networks in silver-based metal-organoboron frameworks. *Chem. Commun.*, 46, 2608-2610.
- Lu, X., Ye, J., Zhang, D., Xie, R., Bogale, R.F., Sun, Y., Zhao, L., Zhao, Q., Ning, G., 2014. Silver carboxylate metal-organic frameworks with highly antibacterial activity and biocompatibility. *J Inorg Biochem.*, 138, 114-121.
- Macfie, S.M., Tarmohamed, Y., Welbourn, P.M., 1994. Effects of cadmium, cobalt, copper, and nickel on growth of the green alga *Chlamydomonas reinhardtii*: The influences of the cell wall and pH. *Archives of Environ. Contam. Toxicol.*, 27, 454-458.
- Macfie, S.M., Welbourn, P.M., 2000. The cell wall as a barrier to uptake of metal ions in the unicellular green alga *Chlamydomonas reinhardtii* (Chlorophyceae). *Arch. Environ. Contam. Toxicol.*, 39, 413-419.
- Marker, A.F.H., 1972. The use of acetone and methanol in the estimation of chlorophyll in the presence of phaeophytin. *Freshwater Biol.*, 2, 361-385.
- Martin, K., Rodea, I., Munoz, M.A., Leganes, F., Fernandez-Pinas, F., 2015. Construction of a self-luminescent cyanobacterial bioreporter that detects a broad range of bioavailable heavy metals in aquatic environments. *Front. Microbiol.*, 6, 186.
- Matsumura, Y., Yoshikata, K., Kunisaki, S., Tsuchido, T., 2003. Mode of bactericidal action of silver zeolite and its comparison with that of silver nitrate. *Appl. Environ. Microbiol.*, 69, 4278-4281.
- McKinlay, A.C., Morris, R.E., Horcajada, P., Férey, G., Gref, R., Couvreur, P., Serre, C., 2010. BioMOFs: Metal-organic frameworks for biological and medical applications. *Angew. Chem. Int. Ed.*, 49, 6260-6266.
- Merlino, J., Kennedy, P., 2010. Resistance to the biocidal activity of silver in burn wound dressings – is it a problem? *Microbiol. Aust.*, 31, 168-170.
- Mieszkin, S., Callow, M.E., Callow, J.A., 2013. Interactions between microbial biofilms and marine fouling algae: a mini review. *Biofouling*, 29, 1097-1113.
- Navarro, E., Piccapietra, F., Wagner, B., Marconi, F., Kaegi, R., Odzak, N., Sigg, L., Behra, R., 2008. Toxicity of silver nanoparticles to *Chlamydomonas reinhardtii*. *Environ. Sci. Technol.*, 42, 8959-8964.
- Nguyen, T., Roddick, F.A., Fan, L., 2012. Biofouling of water treatment membranes: a review of the underlying causes, monitoring techniques and control measures. *Membranes*, 2, 804-840.
- Palza, H., Delgado, K., Curotto, N., 2015. Synthesis of copper nanostructures on silica-based particles for antimicrobial organic coatings. *Appl. Surf. Sci.*, 357, 86-90.
- Paquin, P.R., Gorsuch, J.W., Apte, S., Batley, G.E., Bowles, K.C., Campbell, P.G., Delos, C.G., Di Toro, D.M., Dwyer, R.L., Galvez, F., Gensemer, R.W., Goss, G.G., Hogstrand, C., Janssen, C.R., McGeer, J.C., Naddy, R.B., Playle, R.C., Santore, R.C., Schneider, U., Stubblefield, W.A., Wood, C.M., Wu, K.B., 2002. The biotic ligand model: a historical overview. *Comp. Biochem. Physiol. C Toxicol. Pharmacol.*, 133, 3-35.
- Phan, A., Doonan, C.J., Uribe-Romo, F.J., Knobler, C.B., O'Keeffe, M., Yaghi, O.M., 2010. Synthesis, structure, and carbon dioxide capture properties of zeolitic imidazolate frameworks. *Acc. Chem. Res.*, 43, 58-67.
- Prince, J.A., Bhuvana, S., Anbharasi, V., Ayyanar, N., Boodhoo, K.V., Singh, G., 2014. Self-cleaning Metal Organic Framework (MOF) based ultra filtration membranes. A solution to bio-fouling in membrane separation processes. *Sci. Rep.*, 4, 6555.
- Quirós, J., Boltes, K., Aguado, S., de Villoria, R.G., Vilatela, J.J., Rosal, R., 2015. Antimicrobial metal-organic frameworks incorporated into electrospun fibers. *Chem. Eng. J.*, 262, 189-197.
- Quirós, J., Gonzalo, S., Jalvo, B., Boltes, K., Perdigon-Melon, J.A., Rosal, R., 2016. Electrospun cellulose acetate composites containing supported metal nanoparticles for antifungal membranes. *Sci. Total Environ.*, 563-564, 912-920.
- Rai, M., Yadav, A., Gade, A., 2009. Silver nanoparticles as a new generation of antimicrobials. *Biotechnol. Adv.*, 27, 76-83.
- Refat, M.S., El-Korashy, S.A., Ahmed, A.S., 2008. Preparation, structural characterization and biological evaluation of l-tyrosinate metal ion complexes. *J. Molec. Struct.*, 881, 28-45.
- Rippka, R., 1988. Isolation and purification of cyanobacteria. *Methods Enzymol.*, 167, 3-27.
- Rodea-Palomares, I., Boltes, K., Fernandez-Pinas, F., Leganes, F., Garcia-Calvo, E., Santiago, J., Rosal, R., 2011. Physicochemical characterization and ecotoxicological assessment of CeO₂ nanoparticles using two aquatic microorganisms. *Toxicol. Sci.*, 119, 135-145.
- Rosenhahn, A., Schilp, S., Kreuzer, H.J., Grunze, M., 2010. The role of "inert" surface chemistry in marine biofouling prevention. *Phys. Chem. Chem. Phys.*, 12, 4275-4286.
- Rueff, J.M., Perez, O., Caignaert, V., Hix, G., Berchel, M., Quentel, F., Jaffrès P.A., 2015. Silver-based hybrid materials from meta- or para-phosphonobenzoic acid: influence of the topology on silver release in water. *Inorg. Chem.*, 54, 2152-2159.
- Ruyra, A., Yazdi, A., Espin, J., Carne-Sánchez, A., Roher, N., Lorenzo, J., Imaz, I., MasPOCH, D., 2015. Synthesis, culture medium stability, and in

- vitro and in vivo zebrafish embryo toxicity of metal-organic framework nanoparticles. *Chem. Eur. J.*, 21, 2508–2518.
- Salta, M., Wharton, J.A., Blache, Y., Stokes, K.R., Briand, J.F., 2013. Marine biofilms on artificial surfaces: structure and dynamics. *Environ Microbiol.*, 15, 2879-2893.
- Sancet, M.P., Hanke, M., Wang, Z., Bauer, S., Azucena, C., Arslan, H.K., Heinle, M., Gliemann, H., Wöll, C., Rosenhahn, A., 2013. Surface anchored metal-organic frameworks as stimulus responsive antifouling coatings. *Biointerphases*, 8, 29.
- Sánchez, M.J., Mauricio, J.E., Paredes, A.R., Gamero, P., Cortés, D., 2017. Antimicrobial properties of ZSM-5 type zeolite functionalized with silver. *Mater. Lett.*, 191, 65–68.
- Schultz, M.P., Bendick, J.A., Holm, E.R., Hertel, W.M., 2011. Economic impact of biofouling on a naval surface ship. *Biofouling*, 27, 87-98.
- Sondi, I., Salopek-Sondi, B., 2004. Silver nanoparticles as antimicrobial agent: a case study on *E. coli* as a model for Gram-negative bacteria. *J Colloid Interface Sci.*, 275, 177-182.
- Spokoyny, A.M., Kim, D., Sumrein, A., Mirkin, C.A., 2009. Infinite coordination polymer nano- and microparticle structures. *Chem. Soc. Rev.*, 38, 1218-1227.
- Tsoukatou, M., Hellio, C., Vagias, C., Harvala, C., Roussis, V., 2002. Chemical defense and antifouling activity of three Mediterranean sponges of the genus *Ircinia*. *Z. Naturforsch. C.*, 57, 161-171.
- Wang, C., Qian, X., An, X., 2015. In situ green preparation and antibacterial activity of copper-based metal-organic frameworks/cellulose fibers (HKUST-1/CF) composite. *Cellulose*, 22, 3789-3797.
- Wojciechowska, A., Gagor, A., Wysokinski, R., Trusz-Zdybek, A., 2012. Synthesis, structure and properties of $[Zn(L-Tyr)_2(bpy)]_2 \cdot 3H_2O \cdot CH_3OH$ complex: Theoretical, spectroscopic and microbiological studies. *J Inorg Biochem.*, 117, 93-102.
- Wyszogrodzka, G., Marszalek, B., Gil, B., Dorozynski, P., 2016. Metal-organic frameworks: mechanisms of antibacterial action and potential applications. *Drug. Discov. Today.*, 21, 1009-1018.
- Yaghi, O.M., O'Keeffe, M., Ockwig, N.W., Chae, H.K., Eddaoudi, M., Kim, J., 2003. Reticular synthesis and the design of new materials. *Nature*, 423, 705-714.
- Zhang, J.-P., Lin, Y.-Y., Huang, X.-C., Chen, X.-M., 2005. Copper(I) 1,2,4-triazolates and related complexes: Studies of the solvothermal ligand reactions, network topologies, and photoluminescence properties. *J. Amer. Chem. Soc.*, 127, 5495-5506.
- Zhao, C.M., Campbell, P.G.C., Wilkinson, K.J., 2016. When are metal complexes bioavailable? *Environ. Chem.*, 13, 425–433.
- Zhou, Y., Deng, Y., He, P., Dong, F., Xia, Y., He, Y., 2014. Antibacterial zeolite with a high silver-loading content and excellent antibacterial performance. *RSC Adv.*, 4, 5283–5288.
- Zhuang, W., Yuan, D., Li, J.R., Luo, Z., Zhou, H.C., Bashir, S., Liu, J., 2012. Highly potent bactericidal activity of porous metal-organic frameworks. *Adv. Healthc. Mater.*, 1, 225-238.

SUPPLEMENTARY MATERIAL

Co, Zn and Ag-MOFs evaluation as biocidal materials towards photosynthetic organisms

Georgiana Amariei¹, Karina Boltes^{1,2,*}, Roberto Rosal^{1,2}, Pedro Letón^{1,2}, Keila Martín-Betancor¹, Sonia Aguado², Ismael Rodea-Palomares¹, Miguel Tamayo-Belda¹, Francisco Leganés¹, Roberto Rosal², Francisca Fernández-Piñas^{1,*}

¹ Department of Biology, Facultad de Ciencias, Universidad Autónoma de Madrid, 28049 Madrid, Spain

² Department of Chemical Engineering, Universidad de Alcalá, Alcalá de Henares, 28871 Madrid, Spain

* Corresponding author: francisca.pina@uam.es

Supplementary text. Preparation of materials.

Zn-SIM-1 synthesis. In a typical synthesis a solid mixture of 0.179 g (0.68 mmol) of Zn(NO₃)₂·4H₂O and 0.301 g (2.7 mmol) of 4-methyl-5-imidazolecarboxaldehyde is dissolved in 5 ml of DMF. Afterwards the solution is poured into a vial and heated in an oven at 373 K for 72 h. After the synthesis, the resulting powder is washed 3 times with DMF then with EtOH. The samples are dried at 373K overnight. Empirical formula C₁₀H₁₀ZnN₄O₂

Co-SIM-1 synthesis. In a typical synthesis a solid mixture of 0.199 g (0.68 mmol) of Co(NO₃)₂·6H₂O and 0.301 g (2.7 mmol) of 4-methyl-5-imidazolecarboxaldehyde is dissolved in 5 ml of DMF. Afterwards the solution is poured into a vial and heated in an oven at 358 K for 72 h. After the synthesis, the resulting powder is washed 3 times with DMF then with EtOH. The samples are dried at 373K overnight. Empirical formula C₁₀H₁₀CoN₄O₂

AgTAZ synthesis. A mixture of AgNO₃ (1.70 g, 10 mmol), aqueous ammonia (25%, 20 mL), and 1,2,4-triazole (0.69 g, 10 mmol) was sealed in a 45 mL Teflon-lined reactor and heated in an oven at 373 K for 60 h. After the synthesis, the resulting powder is washed 3 times with EtOH. The samples are dried at 373K overnight. Empirical formula C₂H₂AgN₃

Table S1. Composition of media for culture of *Synechococcus* (BG11), *Anabaena* (AA/8 + N) and *Chlamydomonas* (TAP-).

BG11*		AA/8 + N*		TAP-*	
Compound	Concentration (μM)	Compound	Concentration (μM)	Compound	Concentration (μM)
NaNO ₃	18000	MgSO ₄	125	NH ₄ CL	7015
MgSO ₄	200	CaCl ₂	62.5	MgSO ₄	831
CaCl ₂	240	NaCl	500	CaCl ₂	454
K ₂ HPO ₄	230	K ₂ HPO ₄	250	K ₂ HPO ₄	0.62
EDTA	2.80	NaNO ₃	2500	KH ₂ PO ₄	0.39
Citric acid	31	KNO ₃	2500	NO ₃	211
Ammonium ferric citrate	20	Na ₂ EDTA	9.59375	PO ₄ ³⁻	17.72
Na ₂ CO ₃	190	FeSO ₄	8.645	Fe	10.66
H ₃ BO ₃	46	MnCl ₂	1.13625	Zn	0.47
MnCl ₂	9.1	MoO ₃	0.15625	Mn	0.47
ZnSO ₄	0.77	ZnSO ₄	0.095625	Mo	0.34
Na ₂ MoO ₄	1.6	CuSO ₄	0.0395	Co	0.05
CuSO ₄	0.32	H ₃ BO ₃	5.78125	Cu	0.047
Co(NO ₃) ₂	0.17	NH ₄ VO ₃	0.0245	Thiamine HCL	0.026
MOPS	2 (mM)	CoCl ₂	0.021	Biotin	0.002
				Cyanocobalamim	0.00036

*Adjusted to pH 7.5

Table S2. Metal dissolved concentration released from 50 mg L⁻¹ of each MOF calculated by ICP-MS after 24 h of exposure in each medium and percentage of main species predicted by VISUAL MINTEQ.

Medium		BG11		AA/8+N		TAP-
MOFs	Metal dissolved calculated by ICP-MS (mg L ⁻¹)	Main species predicted by VISUAL MINTEQ (%)	Metal dissolved calculated by ICP-MS (mg L ⁻¹)	Main species predicted by VISUAL MINTEQ (%)	Metal dissolved calculated by ICP-MS (mg L ⁻¹)	Main species predicted by VISUAL MINTEQ (%)
Ag-TAZ	0.1896	57.439 Ag ⁻ 40.040 AgCl 2.001 AgCl ₂ ⁻ 0.119 AgSO ₄ ⁻ 0.399 AgNO ₃	0.0128	49.016 Ag ⁻ 47.489 AgCl 2.984 AgCl ₂ ⁻ 0.403 AgSO ₄ ⁻ 0.104 AgNO ₃	0.3158	2.187 Ag ⁻ 41.251 AgCl 55.498 AgCl ₂ ⁻ 1.025 AgCl ₃ ²⁻ 0.039 AgCl ₄ ³⁻
Zn-SIM1	2.4073	26.287 Zn ²⁺ 0.020 ZnCl ⁺ 11.150 ZnOH ⁺ 0.237 Zn(OH) ₂ 0.338 ZnSO ₄ 0.031 ZnH ₂ PO ₄ ⁺ 2.699 ZnHPO ₄ 0.679 ZnNO ₃ ⁺ 0.311 ZnHCO ₃ ⁺ 0.677 ZnCO ₃ 54.503 Zn-CITRATE 3.046 Zn-EDTA ²⁻	2.556	43.571 Zn ²⁺ 0.051 ZnCl ⁺ 21.291 ZnOH ⁺ 0.475 Zn(OH) ₂ 0.018 ZnOHCl 2.696 ZnSO ₄ 0.077 ZnH ₂ PO ₄ ⁺ 7.024 ZnHPO ₄ 0.378 ZnNO ₃ ⁺ 0.015 Zn(SO ₄) ₂ ²⁻ 24.402 Zn-EDTA ²⁻	2.4033	68.542 Zn ²⁺ 1.425 ZnCl ⁺ 28.479 ZnOH ⁺ 0.590 Zn(OH) ₂ 0.468 ZnOHCl 0.464 ZnHPO ₄ 0.021 ZnNO ₃ ⁺
Co-SIM1	8.4586	98.324 Co ²⁺ 1.676 Co-EDTA ²⁻	10.7365	95.380 Co ²⁺ 4.620 Co-EDTA ²⁻	12.2019	100.000 Co ²⁺

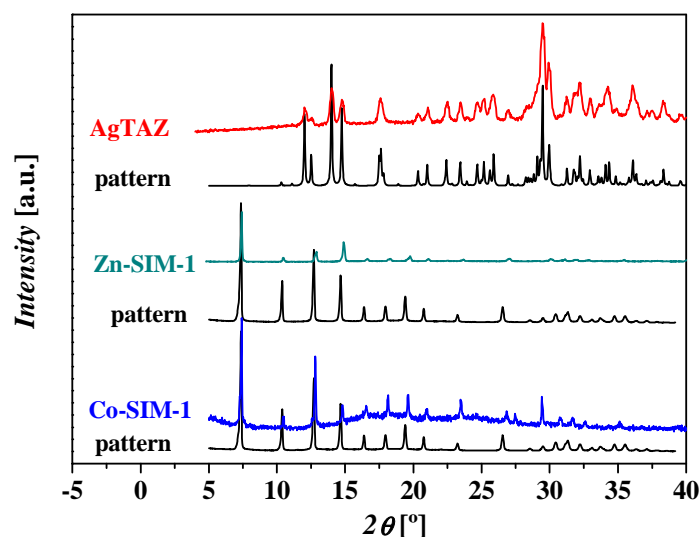


Figure S1. XRD patterns of Ag-TAZ, Zn-SIM1 and Co-SIM1. The XRD measurements on the materials were recorded in the 10–90° 2θ range (scan speed = 20 s, step = 0.04°) by powder X-Ray diffraction (PXRD) using a Shimadzu 600 Series Diffractometer employing CuKα radiation (λ=1.5418 Å).

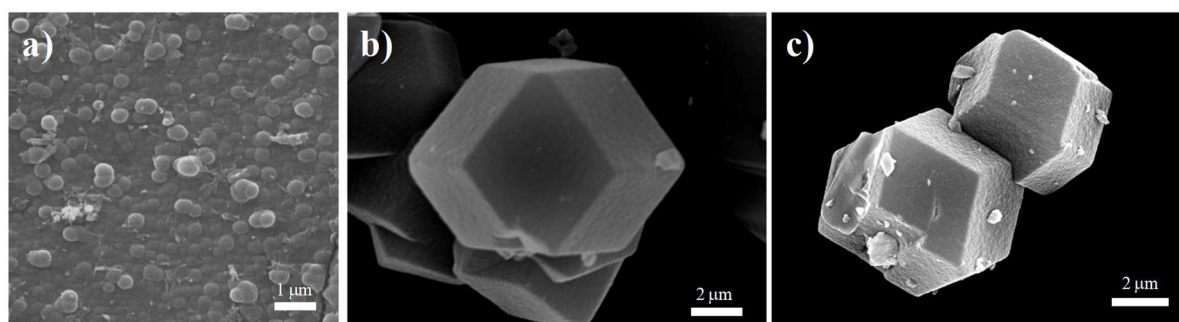


Figure S2. SEM pictures of Ag-TAZ, Zn-SIM1 and Co-SIM1. The morphology of the as-synthesized materials was examined by scanning electron microscopy (SEM) using a DSM-950 (Zeiss) microscope.